Accepted Manuscript

Title: Cell Response to Plasma Electrolytic Oxidation Surface-Modified Low-Modulus β-Type Titanium Alloys

Authors: C.E. Tanase, M. Golozar, S.M. Best, R.A. Brooks

Please cite this article as: Tanase CE, Golozar M, Best SM, Brooks RA, Cell Response to Plasma Electrolytic Oxidation Surface-Modified Low-Modulus β-Type Titanium Alloys, *Colloids and Surfaces B: Biointerfaces* (2018), https://doi.org/10.1016/j.colsurfb.2018.12.064

This is a PDF file of an unedited manuscript that has been accepted for publication. As a service to our customers we are providing this early version of the manuscript. The manuscript will undergo copyediting, typesetting, and review of the resulting proof before it is published in its final form. Please note that during the production process errors may be discovered which could affect the content, and all legal disclaimers that apply to the journal pertain.

Cell Response to Plasma Electrolytic Oxidation Surface-Modified Low-Modulus β-Type Titanium Alloys
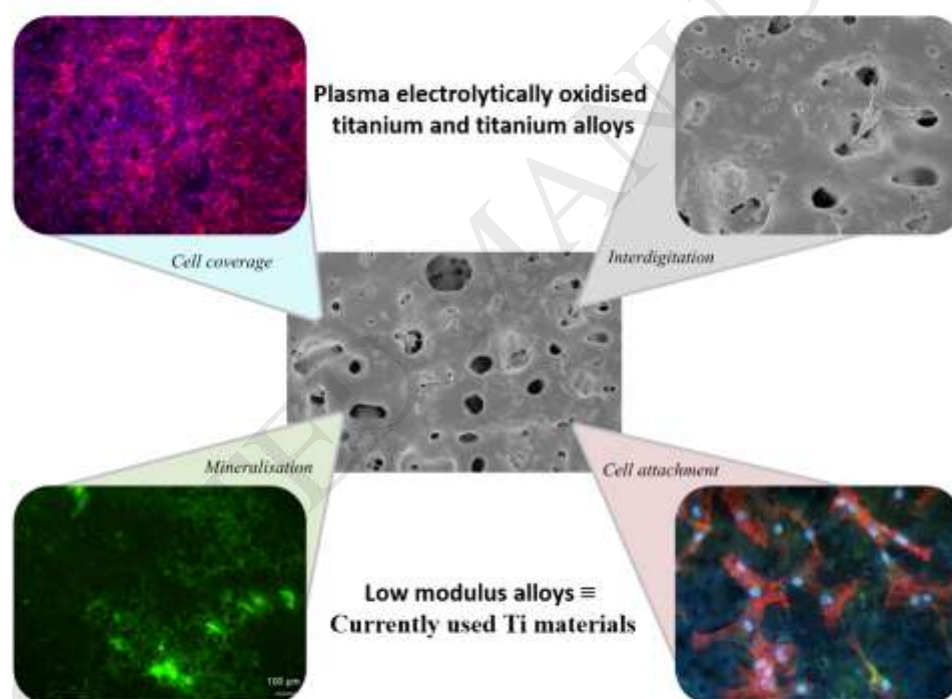
C.E. Tanase[1*], M. Golozar[2], S.M. Best[2] and R.A. Brooks[1*]

[1]Division of Trauma & Orthopaedic Surgery, University of Cambridge, CB2 0QQ, United Kingdom

[2]Cambridge Centre for Medical Materials, Department of Materials Science & Metallurgy, University of Cambridge, CB3 0FS United Kingdom

*cetanase@cantab.net; rb10003@cam.ac.uk

Graphical abstract

Highlights:

- PEO application to β-type titanium alloys for load-bearing orthopaedic implants
- PEO treated samples promote osteoblast attachment, spreading and apatite deposition
- Cell interdigitation into the porous structure of the coatings was observed

- PEO does not impede osteoblast activity or induce an untoward inflammatory response

ABSTRACT

Plasma electrolytic oxidation (PEO) has been demonstrated to be an effective surface treatment for enhancing the osteoconduction and osseointegration of commercially pure α-Ti (CP α-Ti) dental implant materials for clinical application. To explore the feasibility of extending the application of PEO to low-modulus β-type titanium alloys for load-bearing orthopaedic implants, a thorough understanding of the effect of substrate material on the biological performance of the PEO-treated surface is required. A 10 kW 50 Hz KeroniteTM processing unit was used to modify the surface of low-modulus near β-Ti13Nb13Zr and β-Ti45Nb substrates. CP α-Ti and (α+β)-Ti6Al4V were also used in parallel as reference materials. *In vitro* culture of foetal human osteoblast (fHOb) cells on PEO-treated low-modulus near β-Ti13Nb13Zr and β-Ti45Nb alloys revealed comparable behaviour to that seen with CP α-Ti and (α+β)-Ti6Al4V with respect to metabolic activity, collagen production, matrix formation and matrix mineralisation. No difference was observed in TNF-α and IL-10 cytokine release from CD14+ monocytes as markers of inflammatory response across samples. Cell interdigitation into the porous structure of the PEO coatings was demonstrated and cell processes remained adherent to the porous structure despite rigorous sonication. This study shows that PEO technology can be used to modify the surface of low-modulus β-type titanium alloys with porous structure facilitating osseointegration, without impeding osteoblast activity or introducing an untoward inflammatory response.

Introduction

In order to optimise the osseointegration of implanted biomaterials, an in-depth understanding of the physical and chemical characteristics of the bone–implant interface is required, since attributes such as surface topography and chemistry play an important role in cell attachment, spreading and proliferation as well as the initial inflammatory response[1–3]. The mechanisms underpinning the interactions between the implant and the surrounding cells are still the subject of considerable interest and debate; however, several studies have shown that osseointegration can be improved by modifying the surface roughness of the implanted biomaterial[2,4–6]. Following implantation, the surface of the implant comes into contact with a number of proteins and cell types, including neutrophils, monocytes, macrophages, stromal cells and osteoblasts, which is in turn affected by the surface physicochemical properties of the implant material such as roughness, wettability, and porosity. Therefore, the cell behaviour at the bone–implant interface is influenced by the biomaterial surface characteristics[7,8] which, in turn, influence the outcome of the implantation procedure [9].

Metals are probably still the materials most frequently used in orthopaedic surgery for bone interfacing applications including fracture fixation, and reconstructions of damaged tissue in patients with degenerative and inflammatory conditions of bone and joints. Thus, metallic biomaterials must exhibit specific properties such as biological compatibility, enhanced mechanical performance and superior corrosion resistance[10,11]. Titanium and titanium alloys are of particular interest due to the passive titanium oxide layer that forms readily on their surface when exposed to the atmosphere providing corrosion resistance and chemical stability[12,13]. This native oxide layer is thin (approximately 2-7 nm) and bioinert, but its ability to induce apatite formation is dependent on the surface properties of the oxide layer, rather than on the bulk titanium itself[14]. Several methods have been used to introduce a bioactive layer to promote long-term osseointegration[15–18]. Plasma electrolytic oxidation (PEO), also called anodic spark oxidation or micro-arc oxidation, has been shown over the last decade to be a highly effective methods to produce a bioactive surface with a rough and porous structure. The coating layer produced using PEO has been shown extensively to enhance the bioactivity and osseointegration of commercially pure α-Ti (CP α-Ti) dental implant materials, e.g. TiUnite® (Nobel Biocare)[19–21], BioSpark™ (Keystone Dental)[22–27], and Ticer® (ZL Microdent)[28,29].

A wide variety of low-modulus β-type titanium alloys have been developed for potential use in load-bearing orthopaedic applications to ameliorate the effects of stress shielding on bone[30–33]; however, the applicability of PEO treatment to low-modulus titanium alloys in a long term *in vitro* study has not yet been investigated. Hence, we considered

3

that knowledge transfer of the PEO technique from CP α-Ti to low-modulus β-type titanium alloys would be a valuable assessment for orthopaedic research. The aim of this work was to explore the effect of PEO-treated near β- and β-type titanium alloys compared with PEO-treated CP α-Ti and (α+β)-Ti6Al4V on foetal human osteoblasts (fHOb) and investigate the early inflammatory response using $CD14^+$ monocytes.

Materials and methods

PEO COATING PREPARATION

Coatings were produced on four different titanium and titanium alloy substrates: CP α-Ti (Ti-TEK Ltd., Birmingham, UK), (α+β)-Ti6Al4V (Ti-TEK Ltd., Birmingham, UK), near β-Ti13Nb13Zr (Xi'an Saite Metal Materials Development Co., Ltd., Xi'an, Shaanxi, China), and β-Ti45Nb (ATI WahChang, Huntsville, USA). CP α-Ti and (α+β)-Ti6Al4V are the most commonly used substrate materials in dentistry and orthopaedics, respectively, and these served as commercial reference materials for comparison with the low-modulus near β-Ti13Nb13Zr and β-Ti45Nb. The substrates were cut into discs (9 mm diameter and 1 mm thickness) using an Accutom-5 (Struers), ground using P400, P600, P800, P1200 and P2500 grit SiC abrasive papers on a Rotopol system (Struers), and then ultrasonicated in acetone and deionised water (30 min each) to remove debris. To avoid surface contamination, discs were handled using forceps and gloved hands. PEO was conducted in a 10 kW 50 Hz AC Keronite^{TM} processing unit composed of a series of variable capacitor banks that were charged using a three-phase supply, and with the effective capacitance adjusted to maintain a current density of approximately 20 A dm^{-2} throughout the PEO process. A dilute aqueous sodium phosphate electrolyte was used (0.05 M $Na_3PO_4 \cdot 12H_2O$). The electrolyte temperature was maintained at 18±2°C by recirculation through a heat exchanger, with a whistle pump continuously agitating and aerating the electrolyte. PEO processing time points of 2, 5 and 30 min were selected for biological evaluation of the coatings. Untreated (bare) substrates were also used in parallel as controls (t_{PEO}: 0 min). Specimens were cleaned for 15 min in 100% ethanol and sterilised in a hot air oven at 230°C for 2 hours prior to cell culture experiments.

BIOLOGICAL EVALUATION OF PEO COATINGS
Cell Culture

A 26-day cell culture experiment with the addition of osteogenic stimuli was performed to evaluate the behaviour of differentiated osteoblasts on PEO-treated titanium and titanium alloys, including the measurement of matrix formation and mineralisation. The fHOb (406-05f) were obtained from Public Health England Culture Collections. The fHOb are derived from normal foetal bone and express markers found in human bone marrow stromal cells[34]. They provide a suitable model system for studying osteoblast function and differentiation in response to PEO-treated titanium and titanium alloys intended for use as endosseous implants[25,26,35,36]. The fHOb were cultured in Dulbecco's modified Eagle medium (DMEM), low glucose, supplemented with 10% (v/v) foetal bovine serum (FBS), 10,000 units mL^{-1} penicillin, 10 mg mL^{-1} streptomycin, and 30 μg mL^{-1} vitamin C (growth medium). All reagents used for the cell culture experiments were obtained from Invitrogen^{TM} Life Technologies, unless otherwise indicated. Cells were maintained under standard cell culture conditions, including 5% CO_2, 95% humidity and 37°C. They were allowed to proliferate until reaching 70-80% confluency, at which point they were passaged. Cells were detached from the substrates using TrypLE^{TM} and centrifuged at 250 ×G to pellet the cells before resuspension in fresh culture medium. The fHOb were passaged five times prior to cell culture experiments.

Flasks containing subconfluent cultures were treated with TrypLE^{TM} to detach the cells, which were counted using a Cell Scepter^{TM} (Millipore) and seeded onto each substrate in 1 ml of medium at a density of 0.5×10^4 cells cm^{-2} in 48 well culture plates. After adding the cells, plates were shaken gently and centrifuged at 300 ×G for 10 min to sediment cells onto the discs, which were then carefully transferred to a new 48-well plate containing complete medium. Cells were maintained under standard cell culture conditions (5% CO_2, 95% humidity and 37°C). At predetermined time points (1, 3, 6, 9, 13, 16, 19, 22 and 26 days) the medium was changed, and the removed medium stored at -80°C for further analysis. To evaluate cell mineralisation, osteogenic supplements were added to the medium starting from day 16 to induce osteoblast differentiation of the fHOb. The osteogenic medium was growth medium with the addition of 200 nM hydrocortisone and 2 mM β-glycerophosphate. Osteoblast function was evaluated by measuring metabolic activity (alamarBlue® assay) and collagen production (Immuno-dot Blot assay) after 1, 3, 6, 9, 13, 16, 19, 22 and 26 days and matrix mineralisation (OsteoImage^{TM} and Alizarin Red S) at day 26.

alamarBlue®Assay

5

The cell metabolic activity of the fHOb was monitored using the alamarBlue® assay (AbDSerotec) at predetermined time points. In the alamarBlue® assay, the reducing environment produced by the metabolic activity of the cells brings about the reduction of resazurin, a non-fluorescent blue dye, to the highly fluorescent red resorufin. The assay was carried out according to the manufacturer's protocol. In brief, medium was removed from the cells and fresh medium containing 10% (v/v) alamarBlue® was added to each substrate well. The plate was then incubated for 180 min at 37°C, protected from light. After incubation, 100 µL of medium from each well was transferred in triplicate to a black 96-well plate (Falcon), and read using a FLUOstar Optima (BMG Labtech, Offenburg, Germany) fluorescence plate reader at 530 nm excitation and 590 nm emission. The % reduction of alamarBlue® was calculated using the following equation:

$$\% \text{ reduction of alamarBlue} = \frac{S_{aB}^{x} - S_{aB}^{control}}{S_{aB}^{100\% \, reduced} - S_{aB}^{control}} \times 100$$

where S_{aB}^{x} is the alamarBlue® fluorescence signal of the sample at day x, $S_{aB}^{100\% \, reduced}$ is the fluorescence signal of the 100% reduced alamarBlue®, and $S_{aB}^{control}$ is the fluorescence signal of the control (cultured medium supplemented with 10% alamarBlue® solution). The 100% reduced form of alamarBlue® was produced by autoclaving controls at 121°C for 15 min. For all the experiments 6 replicates of each material were used.

Inflammatory Response

Primary human monocytes were used to test the inflammatory response. The CD14+ human monocytes were isolated from buffy coats (National Blood Service, Cambridge, UK) as reported previously[37] and seeded at a concentration of 1×10^{5} cells per disc. Cytokine production was measured in the supernatant harvested at predetermined time points (6, 12, 24 and 48 hours). The levels of the pro-inflammatory cytokine TNF-α and the anti-inflammatory cytokine IL-10 were determined using a double antibody sandwich ELISA according to the manufacturer's protocol (R&D Systems). As a positive control, CD14+ human monocytes were treated with lipopolysaccharide (LPS) 10 µg mL-1 to evaluate the effect of a pro-inflammatory stimulus. Sample values were determined by comparison to a standard curve and all samples were assayed in triplicate.

Immuno-dot Blot Assay

At predetermined time points, the medium from each well was removed and stored at -80°C for future immuno-dot blotting. The medium was subsequently thawed, diluted 1:1 in phosphate buffered saline (PBS) and filtered through a transfer membrane (Immobilon-P, Millipore Corp., Bedford, MA) using the Bio-Dot Apparatus (Bio-Rad, UK). The membranes were blocked with PBS containing 0.1% Tween-20 and 5% non-fat milk powder (PBSTM) for 1 hour and incubated overnight with the primary antibody, anti-collagen type I rabbit IgG (Rockland 600-4001-103-0.1), diluted 1:1,000 in PBSTM. The following morning, membranes were washed twice with PBSTM and incubated for 2 hours with goat anti-rabbit horseradish peroxidase HRP-conjugated secondary antibody (Pierce 31433) at 1:10,000 dilution in PBSTM. Blots were visualised using the ECL Plus blotting system (GE Healthcare, UK) as per the manufacturer's instructions. Developed films were scanned using a GS-710 Calibrated Imaging Densitometer and analysed using Quantity One software (Bio-Rad, UK).

Alizarin Red S Staining

After 26 days of cell culture, cells were washed with PBS and fixed with 10% paraformaldehyde (Merck) for 15 min at room temperature. Subsequently, cells were stained with 1% (w/v) aqueous solution Alizarin Red S sodium salt (Alfa Aesar) for 10 min. After washing four times with Millipore water, the precipitate was solubilised in 10% cetylpyridinium chloride. The solution was then transferred to a 96-well culture plate and the optical density was read at 620 nm using a FLUOstar Optima microplate reader.

Immunofluorescence Microscopy

Following 18 and 72 hours of culture, cells were washed with PBS and fixed using a solution of 3.7% paraformaldehyde for 10 min. The fixed cells were washed again with PBS and permeabilised with 0.5% Triton X-100 for 10 min. Tetramethylrhodamine isothiocyanate conjugated phalloidin (Pha-TRITC) 0.2 µg mL^{-1} (Sigma, St. Louis, MO, USA) was used to visualise the actin cytoskeleton. Additionally, the top surface of the discs was coated with Fluoroshield antifade mountant containing 4',6-diamidino-2-phenylindole (DAPI) (Vector Laboratories) to stain cell nuclei. For the 18-hour time point wheat germ agglutinin-AlexaFluor488 conjugate was used at a concentration of 5 µg mL^{-1} to stain the cell membranes according to manufacturer's instructions. Samples were examined using a Leica DMRXA2 fluorescence microscope.

Scanning Electron Microscopy (SEM)

7

After 72 hours of culture using PEO-treated and untreated (bare) substrates of titanium and titanium alloys, the medium was removed, cells were washed with PBS, and fixed using 4% glutaraldehyde in 0.1 M PIPES (piperazine-N,N'-bis(ethane sulfonic acid); 1,4-piperazinediethanesulfonic acid) for 3 hours. The fixative was removed and samples were gradually dehydrated in a series of ethanol dilutions (*i.e.* 10, 20, 30, 50, 70, 80, 90 and 100% ethanol) for 10 min each. This gradual dehydration process was important to prevent the cells from lysing and preserve the architecture of the plasma membrane and cytoplasmic projections. Samples were placed in a 1:1 ethanol:hexamethyldisilazane solution for 20 min and then transferred to pure hexamethyldisilazane for 20 min. Finally, the hexamethyldisilazane solution was removed and samples were left to dry in the fume hood. Samples were examined using the FEI Nova NanoSEM^{TM} 450 (Field Emission Gun). To prevent charging, samples were sputter-coated using a Pt target under vacuum conditions.

Statistics

Statistical significance was calculated using one-way ANOVA following Levene's test for equality of variance using SPSS software (Version 21; IBM, Chicago, USA). Tukey's posthoc test was used to determine sample differences that were considered significant at $p < 0.05$.

Results

Osteoblast Metabolic Activity: A Prolonged Time Course with Osteogenic Stimuli

Metabolic activity increased with time on all substrates. Figure 1(a–d) shows a time-dependent reduction of alamarBlue® on low-modulus near β-Ti13Nb13Zr and β-Ti45Nb alloys together with CP α-Ti and (α+β)-Ti6Al4V control materials treated using different PEO processing times (t_{PEO}: 0, 2, 5 and 30 min). A characteristic lag-log growth phase was observed from day 0 to day 6, after which cells reached confluency and a plateau phase was observed. After day 9, metabolic activity increased during a post-confluent expansion phase and continued to rise following the addition of osteogenic medium at day 16. No significant differences were observed between different substrates or PEO processing times, including following the addition of osteogenic medium.
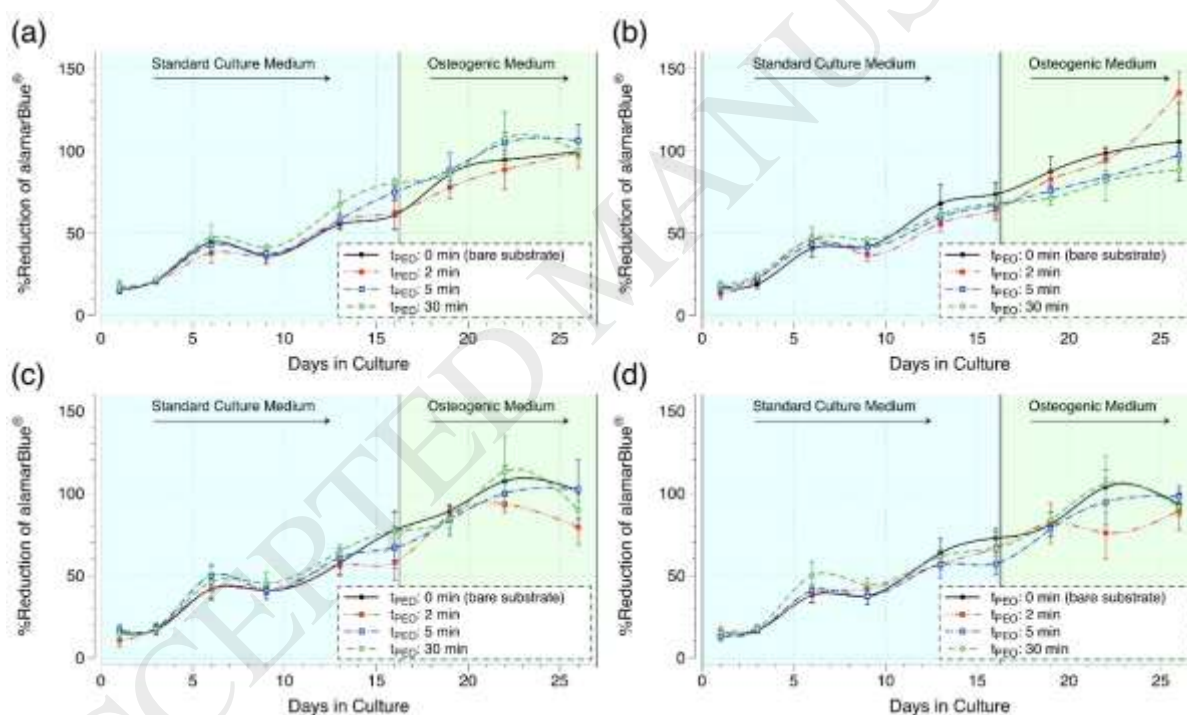

Figure 1: Metabolic activity of fHOb cultured over 26 days on PEO-treated CP α-Ti, (a), (α+β)-Ti6Al4V, (b), near β-Ti13Nb13Zr, (c), and β-Ti45Nb, (d). Cells were cultured in standard culture medium for 16 days, which was subsequently replaced by osteogenic medium for the remainder of the time course. Data represent mean ± SD; n = 6; t_{PEO} = 0, 2, 5 and 30 min of PEO treatment.

Cytokine Release

No significant differences were observed in TNF-α release for either untreated bare substrates (t_{PEO}: 0 min) or PEO-treated substrates (t_{PEO}: 30 min), Figure 2(a-b). A similar

9

behaviour was also observed for the IL-10 release, where there was no significant difference between the responses of the CD14^{+} monocytes cultured on the different modified Ti-based substrates, Figure 2(c-d). Cytokine release was strongly up-regulated by the addition of bacterial lipopolysaccharide (LPS) stimulating CD14^{+} monocytes to release significantly higher levels of TNF-α and IL-10 than untreated cells: 445.05 mg mL^{-1} at 24 hours for TNF-α and 355.85 mg mL^{-1} at 24 hours for IL-10.
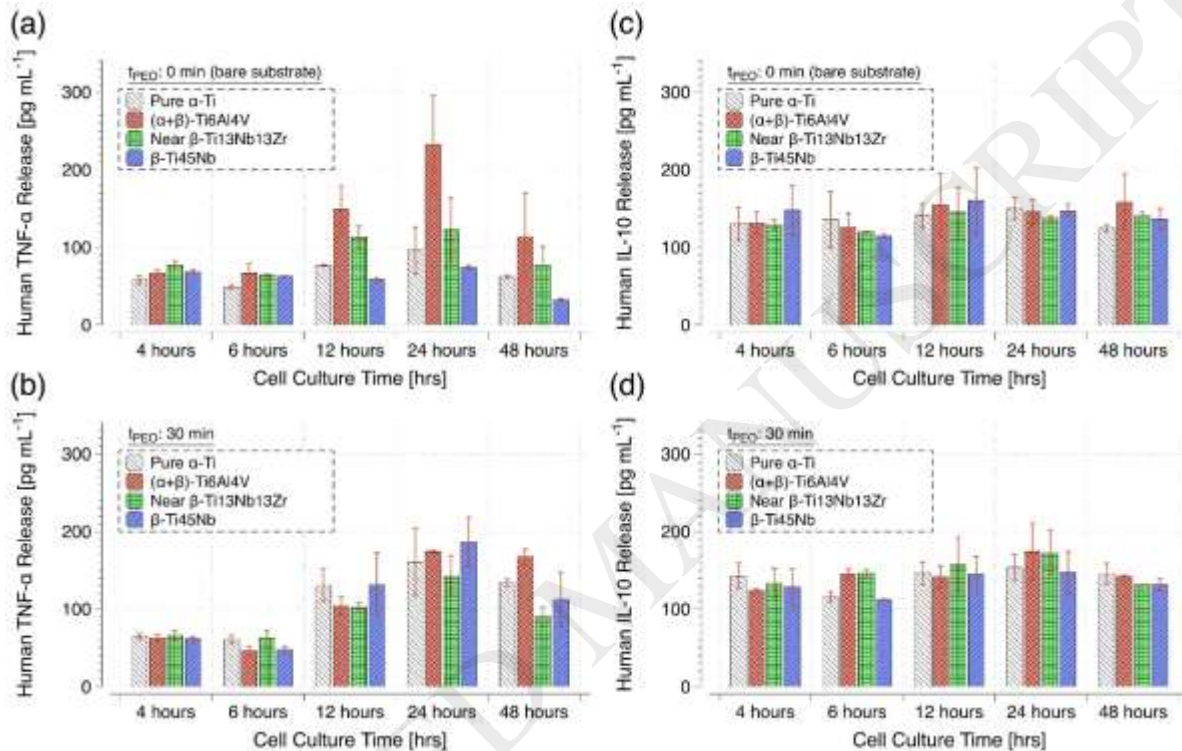

Figure 2: Release of TNF-α (a and b) and IL-10 (c and d) from CD14^{+} monocytes cultured for 48 hours on untreated CP α-Ti, (α+β)-Ti6Al4V, near β-Ti13Nb13Zr, and β-Ti45Nb (a and c) or substrates treated with PEO for 30 minutes (b and d). Data represent mean ± SD; n = 3.

Osteoblast Differentiation: Type-I Collagen Production and Matrix Formation

Figure 3(a–d) presents the production of type I collagen for low-modulus near β-Ti13Nb13Zr and β-Ti45Nb alloys together with the CP α-Ti and (α+β)-Ti6Al4V control materials at different PEO processing time points (t$_{PEO}$: 0, 2, 5 and 30 min). The results showed that collagen production per well continued throughout the 26-day cell culture period with a small decrease in the rate following the addition of osteogenic medium. There was no significant difference in collagen production between osteoblasts cultured on different substrates or for differing lengths of PEO treatment.
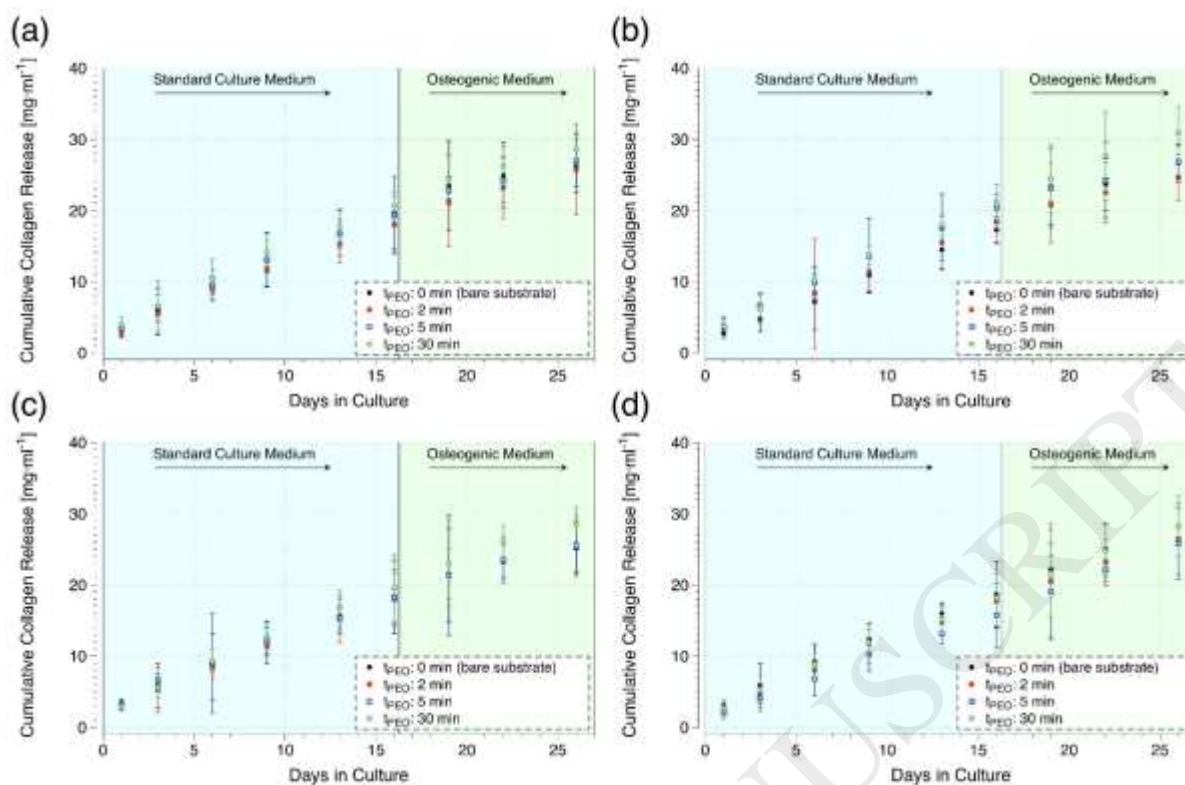
10

Figure 3: Type-I collagen production by fHOb cultured on PEO-treated CP α-Ti, (a), (α+β)-Ti6Al4V, (b), near β-Ti13Nb13Zr, (c), and β-Ti45Nb, (d). Cells were cultured in standard culture medium for 16 days, which was subsequently replaced by osteogenic medium for the remainder of the time course. Data represent mean ± SD; n = 6.

Osteoblast Differentiation: Matrix Mineralisation

Mineralisation, a marker of osteoblast differentiation, can be readily detected in fHOb cultures after 28 days following the addition of osteogenic supplements[38]. In this study, mineralisation was investigated following 26 days of cell culture using two complementary methods: staining calcium deposits with Alizarin Red S and immunofluorescence imaging of hydroxyapatite nodules using OsteoImage[TM]. Figure 4 shows the optical density of Alizarin Red S-stained calcium within hydroxyapatite mineral deposits. There was no significant difference in optical density with PEO processing time. A trend was observed for increased calcium deposition at higher PEO processing times across all four substrate materials; however, this did not reach statistical significance. Representative images of hydroxyapatite nodules on PEO-treated and control surfaces stained at day 26 using OsteoImage[TM] are shown in supplementary figure S1. These demonstrate that the mineral deposited on these surfaces was hydroxyapatite.
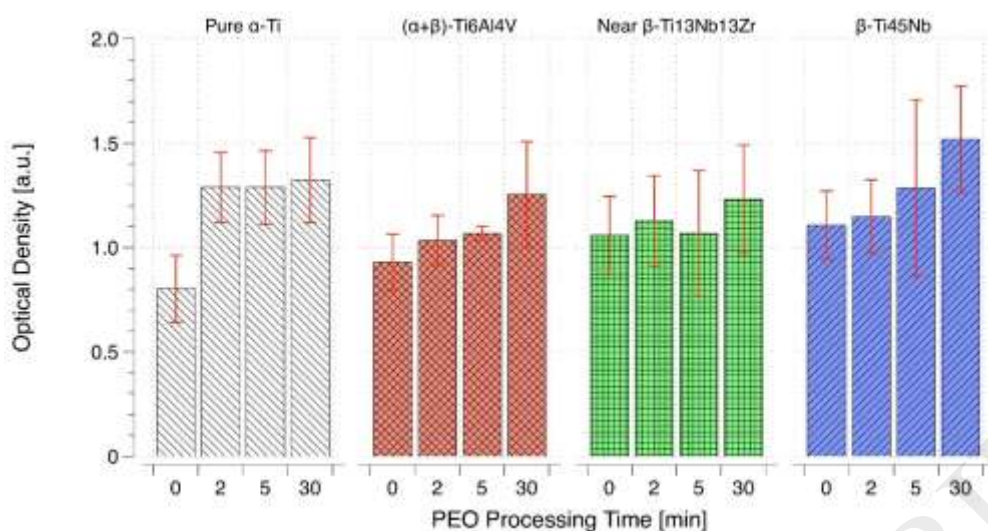
Figure 4: Quantification of Alizarin Red S calcium staining of fHOb cultures grown on PEO-treated low-modulus near β-Ti13Nb13Zr and β-Ti45Nb alloys as well as CP α-Ti and (α+β)-Ti6Al4V control materials after 26 days. Data represent mean ± SD; n = 3.

Osteoblast Distribution, Morphology and Interconnection

The cell distribution and morphology of cultured fHOb after 72 hours on PEO-treated (t_{PEO}: 2, 5 and 30 min) and untreated (bare) substrates were examined using SEM. Suplementary figure S2 shows representative SEM images of cells cultured on on 30 min PEO treated substrates. A uniform monolayer of fHOb was observed showing even spacing between cells with connections between neighbouring cells. The widely spread-out morphology of the cells, with an elongated polygonal shape, is an indication of successful attachment and anchoring to the surface. In particular, the presence of numerous cytoplasmic extensions implies favourable surface adhesion and interaction between cells on the substrate surface. The morphology of the cells appeared similar for all the untreated and PEO-treated substrates regardless of PEO processing time.

Immunofluorescent staining was also carried out on fHOb cultured on PEO-treated and untreated (bare) substrates for 18 hours, Figure 5. At the 18-hour time point, individual cells could be visualised, as they had not yet reached confluency. The cells demonstrated an elongated shape with cytoplasmic projections that stretched to form long-range contact points with neighbouring cells. After 18 hours, there was no perceivable difference in morphology for fHOb, regardless of the substrate material or the PEO processing time points (t_{PEO}: 0, 2, 5 and 30 min). Staining with phalloidin-TRITC showed that all materials effectively supported the formation of an actin cytoskeleton, which enabled the cell to adhere and spread on the substrate surface. After 72 hours in culture the cells showed extensive proliferation and an even

12

distribution of fHOb over the substrate surface for all alloys and all PEO processing time points – supplementary Figure S2. The fHOb were organised into layers of cells, covering almost the entire substrate surface.
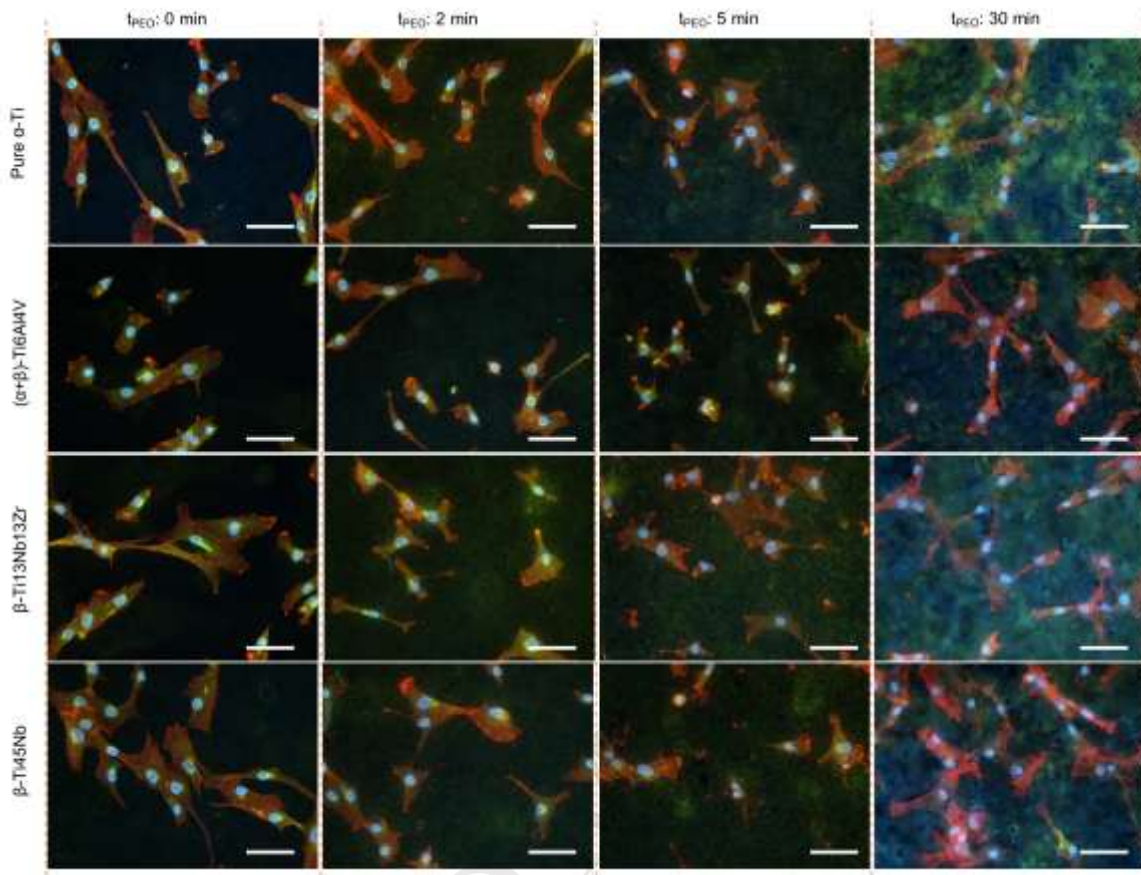

Figure 5: Cell morphology and distribution of fHOb on untreated and PEO-treated substrates after 18 hours in culture; Blue-nuclei, Red-cytoskeleton, and Green-cell membrane (scale bar 100 µm).

PEO enables the formation of rough, porous titanium oxide coatings with a wide range of pore size and distribution (microscale/nanoscale), and therefore, it was hypothesised that cells could display improved interdigitation with the coating through cytoplasmic extension and penetration into the surface pores. A detailed look at the cell–coating interface using SEM revealed evidence of cell interconnection into the porous structure of the PEO coatings, Figure 6. The SEM micrographs show fHObs effectively extending cell processes into the porous structures of PEO-treated near β-Ti13Nb13Zr and β-Ti45Nb substrates (t$_{PEO}$: 30 min).

Discussion

In the present study, we examined the behaviour of fHOb in a prolonged 26-day cell culture experiment on PEO-treated titanium and titanium alloys (t_{PEO}: 0, 2, 5 and 30 min). The alloys were CP α-Ti, (α+β)-Ti6Al4V and the low-modulus materials near β-Ti13Nb13Zr and β-Ti45Nb. In particular, we aimed to determine whether the application of PEO technology could be extended to low-modulus titanium alloys without hindering the osteoblast response or provoking an inflammatory response. The study investigated the behaviour of human osteoblasts on titanium and titanium alloy substrates under osteogenic conditions that induced differentiation, matrix formation and matrix mineralisation as well as evaluating cytokine release from CD14^{+} monocytes.

Microenvironment and proximity to neighbouring cells strongly influence cell behaviour, therefore, it was desirable to maintain a uniform cell distribution across the substrate surface; this was achieved using a centrifugal cell seeding method. Subsequent immunofluorescence and scanning electron microscopy confirmed an even distribution of cells. The fHOb cultured on PEO-treated titanium and titanium alloys exhibited a similar cell morphology to those grown on untreated (bare) substrates presenting an elongated polygonal shape and flattened morphology, displaying numerous cell processes spreading in all directions specifying a close interaction between cells and between cells and their underlying substrates. This represents the standard behaviour of osteoblasts on titanium alloy substrates[9,39]. The cell attachment after 18 hours shows that cells attached to the PEO-treated substrates develop an organised actin cytoskeleton. Cells on both control and PEO-treated samples have parallel or radially oriented actin bundles within the cell body of these cells. Additionally, there was evidence of cell processes extending over other neighbouring cells indicating the formation of cell layering.

The characteristic spreading and morphology of fHOb observed on all four substrate materials and PEO processing times were supported by cell viability measurements using alamarBlue®. Comparable cell metabolic activity was observed for all four PEO-treated titanium and titanium alloys, indicating good cell viability. The increase in metabolic activity up to day 6 is related to the fHOb developing into a confluent monolayer, after which a plateau phase indicates that the metabolic activity of the cultures was stable when confluence had been reached. Some of the increase in metabolic activity in the post confluence expansion phase may have been due to multilayering of cells. The increase in metabolic activity continued after the addition of osteogenic medium and was followed by a second plateau phase on all substrate types after 22 days. This plateau may represent a slowing of cell growth as cells pile up on each

14

other on the substrate surface and nutrients are depleted in the local microenvironment. The PEO processing time did not influence cell metabolic activity indicating that PEO treatment does not have an adverse effect on osteoblast metabolic activity. Additionally, there was no difference between PEO-treated low-modulus near β-Ti13Nb13Zr and β-Ti45Nb alloys compared with PEO-treated CP α-Ti and (α+β)-Ti6Al4V control materials providing initial evidence supporting the development of PEO-treated low-modulus titanium alloys as implant materials.

As fHOb undergo differentiation into mature osteoblasts, they secrete extracellular matrix proteins. The organic component of the extracellular matrix consists mainly of type I collagen with smaller quantities of other proteins. The production of type I collagen is a prerequisite for and precedes the development of mineralised bone. This results in the production of osteoid matrix, which enables the deposition of bone mineral[40]. Collagen type I has also been reported to play an important role in maintaining osteoblast phenotype and stimulating ALP activity[41]. For all materials and PEO processing times, continuous production of type-I collagen was observed during the 26-day culture period. These results suggested that the PEO-treated titanium and titanium alloys supported collagen production and matrix formation although no particular substrate material or PEO processing time was determined to be superior to the others.

The addition of osteogenic medium after day 16 of the 26-day experimental time course permitted the evaluation of mature osteoblast features including matrix mineralisation on the surface of PEO-treated titanium and titanium alloys. The ability of cells to effectively interact with the implant surface and deposit a mineralised matrix is essential to enable subsequent osseointegration. Alizarin Red S measurement and OsteoimageTM staining indicated that there was apatite deposition on the PEO-treated surfaces, however, there was no significant difference with PEO processing time or between low-modulus alloys and control materials. As an aid to future work, we have carried out a power calculation based on the results presented in Figure 4 using a power (1-β) of 0.8 and a type 1 error rate (α) of 5% (www.powerandsamplesize.com), which indicated that a further experiment with at least 5 replicates per group would be required to show whether there is a statistically significant difference between calcium deposition on β-Ti45Nb with 30 min PEO processing compared to untreated β-Ti45Nb and therefore a beneficial effect of PEO processing on mineral deposition.

There are multiple factors that could be involved in promoting osteoblast mineralisation, such as increased PEO coating thickness, coating mass gain, coating surface roughness, and/or coating hydrophilic properties. Previous studies have shown that PEO can

15

be used with no detrimental effect on various titanium based substrates to maintain or even enhance cell function [42–45].

A key attribute of a successful endosseous—dental and orthopaedic—implant is a bioactive surface layer that encourages osteoinduction, osteoconduction and osseointegration for long-term biomechanical stability *in vivo*. Figure 6 illustrates SEM micrographs of cell–coating interdigitation on PEO-treated substrates. There was notable evidence of cell interdigitation after rigorous cleaning and sonication of PEO-treated titanium and titanium alloys, and surprisingly, despite the considerable chemical and physical disruption of cells from the coating surface, cells and cell fragments remained firmly adhered to the coating via interdigitation into the porous structure. This evidence of cell–coating interdigitation may offer enhanced adhesion strength for osteoblasts on the substrate surface[43].

The tissue response at the bone–biomaterial interface following implantation involves cells of the mesenchymal lineage and also an inflammatory response mediated by cytokines secreted from leukocytes[46]. One of the cytokines released at this interface is TNF-α, which is an important signalling molecule involved in the response to foreign materials—its upregulation is considered to be a measure of inflammation[47]. An increase in TNF-α release from cells, which was observed on all untreated (bare) substrates, except β-Ti45Nb and CP α-Ti, is a recognised response to titanium-based biomaterials and may be important in the initial stages of the healing response at the bone–implant interface[48]. For all substrates other than (α+β)-Ti6Al4V and near β-Ti13Nb13Zr, the release of TNF-α was greater from cells on substrates treated with PEO for 30 min compared to untreated (bare) substrates. This may be due to the greater surface roughness as previous studies have shown increased pro-inflammatory cytokine release from cells on titanium alloys with surface roughened by sand blasting and acid etching[48]. Findings related to thermally oxidised or plasma sprayed surfaces revealed that such treatment can alter the inflammatory response by decreasing the TNF-α[49,50]. Our findings did not show this, but the results indicated no significant difference between the PEO-treated and untreated (bare) substrates. When considering an inflammatory process, anti-inflammatory mediators such as IL-10 will concomitantly be found counteracting the pro-inflammatory cytokines[51]. The release of both IL10 and TNF-α from monocytes on titanium and titanium alloys was considerably lower than when cells were cultured with bacterial LPS indicating that there was no untoward inflammatory response to the biomaterials.
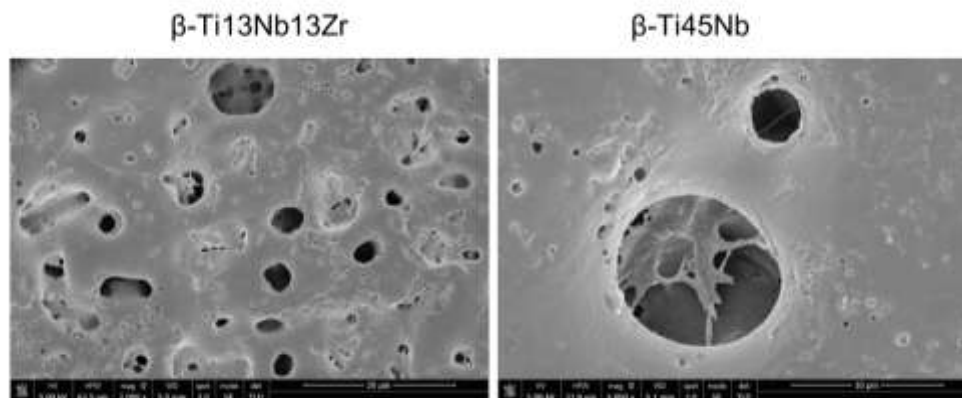
β-Ti13Nb13Zr　　　　　　　　β-Ti45Nb

Figure 6: Typical scanning electron micrographs illustrating cell–coating interdigitation on PEO-treated near β-Ti13Nb13Zr and β-Ti45Nb alloys (t$_{PEO}$: 30 min).

The biological response to titanium and titanium alloys is influenced by the surface physicochemical characteristics of the underlying substrate material[52–54], and although many surface parameters can impact the attachment, adhesion, proliferation and growth of cells[43,45,55,56], in our study metabolic activity and collagen production appeared to be independent of surface chemistry and morphology. The use of PEO on titanium-based biomaterials can help not only to improve wear and corrosion resistance but also to strengthen cellular adhesion[57,58]. Also, in comparison to other competing surface modification technologies, PEO is considered to be more environmentally friendly. Previous studies have also shown that PEO coating composition has an influence on the cell differentiation process and a limited effect on the metabolic activity[59,60], and this could potentially be correlated to the amount of TiO$_2$ anatase phase present within the composition[61]. However, regardless of the anatase phase content of the PEO-treated substrates[62], our results indicate no significant difference in mineralisation for PEO-treated and untreated (bare) substrates similar to previous studies reporting no significant difference between micro-arc oxidised surfaces and untreated (bare) substrates, indicating that both surfaces equally supported cell growth[45]. An in-depth investigation into the surface physical and chemical properties of PEO-treated titanium and titanium alloys is required to better understand the impact of PEO coatings on fHOb biological response.

Predicting how biomaterials may behave *in vivo* is challenging, and thus far, there is no *in vitro* system that is able to meticulously simulate the body condition in every respect. This is largely due to the fact that the *in vivo* microenvironment is immensely more complicated than *in vitro* systems, as it involves complex interactions with other cell types, soluble proteins,

biomolecules, growth factors and biomechanical (load) stimuli within the cell micro/macroenvironment, amongst other factors[63,64]. However, if the results we have obtained *in vitro* were translated into enhanced differentiation and mineralisation *in vivo*, whilst maintaining the required cell proliferation and collagen production, then these materials should improve bone formation and implant fixation at the bone–biomaterial interface.

The results obtained from near β-Ti13Nb13Zr and β-Ti45Nb indicates that PEO is capable of generating bioactive coatings on these alloys with surface features comparable to those of the PEO-treated CP α-Ti implant materials already in use in dentistry, as well as (α+β)-Ti6Al4V. Furthermore, the fHOb response to low-modulus PEO-treated near β-Ti13Nb13Zr and β-Ti45Nb was comparable to CP α-Ti and (α+β)-Ti6Al4V samples, in terms of metabolic activity, morphology, matrix formation and matrix mineralisation. These findings suggest that PEO technology may be extended to novel low-modulus titanium alloys (near β-Ti13Nb13Zr and β-Ti45Nb) without compromising the cellular response. In the context of endosseous orthopaedic implants, the production of a contiguous bone–biomaterial interface using PEO treatment may help facilitate uniform stress transfer from the load-bearing implant using low-modulus β-type titanium alloys to the surrounding bone tissue, minimising the effect of stress shielding, osteolysis and aseptic loosening *in vivo*.

Conclusions

PEO surface modification of low-modulus near β-Ti13Nb13Zr and β-Ti45Nb alloys showed comparable cellular behaviour in a long-term culture to CP α-Ti and (α+β)-Ti6Al4V control substrates. The study also provided evidence of apatite mineral deposition on PEO-treated low-modulus alloys, without an undue inflammatory response. This suggests that PEO application can be successfully extended to modify the surface of low-modulus β-type titanium alloys offering lower stress shielding without impeding the osteoblast response. Cell interdigitation into the porous coatings was also observed, which could potentially improve osseointegration *in vivo*. This work offers valuable guidance for other researchers to pursue these novel PEO-treated low-modulus titanium alloys for further *in vivo* studies and clinical trials.

Acknowledgments

REFERENCES

[1]   D.M. Dohan Ehrenfest, P.G. Coelho, B.S. Kang, Y.T. Sul, T. Albrektsson, Classification of osseointegrated implant surfaces: Materials, chemistry and topography, Trends Biotechnol. 28 (2010) 198–206. doi:10.1016/j.tibtech.2009.12.003.

[2]   A. Göransson, A. Wennerberg, Bone formation at titanium implants prepared with iso- and anisotropic surfaces of similar roughness: an in vivo study., Clin. Implant Dent. Relat. Res. 7 (2005) 17–23. doi:10.1111/j.1708-8208.2005.tb00042.x.

[3]   D. Kubies, L. Himmlová, T. Riedel, E. Chánová, K. Balík, M. Douděrová, J. Bártová, V. Pešáková, The interaction of osteoblasts with bone-implant materials: 1. The effect of physicochemical surface properties of implant materials., Physiol. Res. 60 (2011) 95–111. http://www.ncbi.nlm.nih.gov/pubmed/20945966.

[4]   S. Nayak, T. Dey, D. Naskar, S.C. Kundu, The promotion of osseointegration of titanium surfaces by coating with silk protein sericin., Biomaterials. (2013). doi:10.1016/j.biomaterials.2013.01.019.

[5]   T.J. Webster, J.U. Ejiofor, Increased osteoblast adhesion on nanophase metals: Ti, Ti6Al4V, and CoCrMo., Biomaterials. 25 (2004) 4731–9. doi:10.1016/j.biomaterials.2003.12.002.

[6]   M.J. Dalby, D. McCloy, M. Robertson, C.D.W. Wilkinson, R.O.C. Oreffo, Osteoprogenitor response to defined topographies with nanoscale depths, Biomaterials. 27 (2006) 1306–1315. doi:10.1016/j.biomaterials.2005.08.028.

[7]   J.M. Anderson, A. Rodriguez, D.T. Chang, FOREIGN BODY REACTION TO BIOMATERIALS, Semin. Immunol. 20 (2008) 86–100. doi:10.1016/j.smim.2007.11.004.

[8]   A.M.B. Collie, P.C.S. Bota, R.E. Johns, R. V. Maier, P.S. Stayton, Differential monocyte/macrophage interleukin-1?? production due to biomaterial topography requires the ??2 integrin signaling pathway, J. Biomed. Mater. Res. - Part A. 96 A (2011) 162–169. doi:10.1002/jbm.a.32963.

[9]   K. Anselme, Osteoblast Adhesion on Biomaterials, Biomaterials. 21 (2000) 667–681. doi:10.1016/S0142-9612(99)00242-2.

[10]   M. Niinomi, Mechanical biocompatibilies of titanium alloys for biomedical applications, J. Mech. Behav. Biomed. Mater. 1 (2008) 30–42. doi:http://dx.doi.org/10.1016/j.jmbbm.2007.07.001.

[11]   F. Mahyudin, L. Widhiyanto, H. Hermawan, Biomaterials in orthopaedics, Adv. Struct. Mater. 58 (2016) 161–181. doi:10.1007/978-3-319-14845-8_7.

[12]   M. Geetha, A.K.K. Singh, R. Asokamani, A.K.K. Gogia, Ti based biomaterials, the ultimate choice for orthopaedic implants – A review, Prog. Mater. Sci. 54 (2009) 397–425. doi:10.1016/j.pmatsci.2008.06.004.

[13]   J.J. Jasinski, L. Kurpaska, M. Lubas, M. Lesniak, J. Jasinski, M. Sitarz, Effect of hybrid oxidation on the titanium oxide layer's properties investigated by spectroscopic methods, J. Mol. Struct. 1126 (2015) 165–171. doi:10.1016/j.molstruc.2016.02.080.

[14]   P. Li, C. Ohtsuki, T. Kokubo, K. Nakanishi, N. Soga, K. de Groot, The role of hydrated silica, titania, and alumina in inducing apatite on implants, J. Biomed. Mater. Res. 28 (1994) 7–15. doi:10.1002/jbm.820280103.

[15]   S.R. Paital, N.B. Dahotre, Calcium Phosphate Coatings for Bio-implant Applications: Materials, Performance Factors, and Methodologies, Mater. Sci. Eng. R Reports. 66 (2009) 1–70. doi:10.1016/j.mser.2009.05.001.

[16]   L.T. de Jonge, S.C.G. Leeuwenburgh, J.G.C. Wolke, J.A. Jansen, Organic-inorganic surface modifications for titanium implant surfaces, Pharm. Res. 25 (2008) 2357–2369. doi:10.1007/s11095-008-9617-0.

[17]   G. Mendonça, D.B.S. Mendonça, F.J.L. Aragão, L.F. Cooper, Advancing dental implant surface technology - From micron- to nanotopography, Biomaterials. 29 (2008) 3822–3835.

doi:10.1016/j.biomaterials.2008.05.012.

[18]   P.S. Vanzillotta, M.S. Sader, I.N. Bastos, G. De Almeida Soares, Improvement of in vitro titanium bioactivity by three different surface treatments, Dent. Mater. 22 (2006) 275–282. doi:10.1016/j.dental.2005.03.012.

[19]   T. Jarmar, A. Palmquist, R. Brånemark, L. Hermansson, H. Engqvist, P. Thomsen, Characterization of the Surface Properties of Commercially Available Dental Implants using Scanning Electron Microscopy, Focused Ion Beam, and High-resolution Transmission Electron Microscopy, Clin. Implant Dent. Relat. Res. 10 (2008) 11–22. doi:10.1111/j.1708-8208.2007.00056.x.

[20]   D. French, M. Tallarico, Eight-year Clinical and Radiologic Results of Maxillary and Mandibular Implant-retained Bar Overdentures Carried out on Oxidized (TiUnite^{TM}) Replace Select Implants Placed in Regenerated Bone: A Clinical Case, Quintessence Int. (Berl). 45 (2014) 135–140. doi:10.3290/j.qi.a31012.

[21]   C.A. Babbush, M. Tallarico, Twelve-year Clinical and Radiological Results of Maxillary and Mandibular Implant-retained Bar Overdentures Carried out on Oxidized (TiUnite) Replace Select Implants: A Clinical Case, J. Oral Implantol. 39 (2013) 737–742. doi:10.1563/aaid-joi-d-12-00311.

[22]   G. Giavaresi, M. Fini, R. Chiesa, C. Giordano, E. Sandrini, A.E. Bianchi, P. Ceribelli, R. Giardino, A Novel Multiphase Anodic Spark Deposition Coating for the Improvement of Orthopedic Implant Osseointegration: An Experimental Study in Cortical Bone of Sheep, J. Biomed. Mater. Res. Part A. 85 (2008) 1022–1031. doi:10.1002/jbm.a.31566.

[23]   E. Sandrini, C. Giordano, V. Busini, E. Signorelli, A. Cigada, Apatite Formation and Cellular Response of a Novel Bioactive Titanium, J. Mater. Sci. Mater. Med. 18 (2007) 1225–1237. doi:10.1007/s10856-007-0122-5.

[24]   G. Giavaresi, R. Chiesa, M. Fini, E. Sandrini, Effect of a Multiphasic Anodic Spark Deposition Coating on the Improvement of Implant Osseointegration in the Osteopenic Trabecular Bone of Sheep, Int. J. Oral Maxillofac. Implant. 23 (2008) 659–668.

[25]   E. Sandrini, C. Morris, R. Chiesa, A. Cigada, M. Santin, In Vitro Assessment of the Osteointegrative Potential of a Novel Multiphase Anodic Spark Deposition Coating for Orthopaedic and Dental Implants, J. Biomed. Mater. Res. Part B Appl. Biomater. 73 (2005) 392–399. doi:10.1002/jbm.b.30241.

[26]   N. Bertollo, E. Sandrini, P. Dalla Pria, W.R. Walsh, Osseointegration of Multiphase Anodic Spark Deposition Treated Porous Titanium Implants in an Ovine Model, J. Arthroplasty. 30 (2015) 484–488. doi:10.1016/j.arth.2013.10.003.

[27]   C. Giordano, R. Chiesa, E. Sandrini, A. Cigada, G. Giavaresi, M. Fini, R. Giardino, Physical and Biological Characterizations of a Novel Multiphase Anodic Spark Deposition Coating to Enhance Implant Osseointegration, J. Mater. Sci. Mater. Med. 16 (2005) 1221–1229. doi:10.1007/s10856-005-4732-5.

[28]   H.-L.L. Graf, S. Stoeva, F.P. Armbruster, J. Neuhaus, H. Hilbig, Effect of bone sialoprotein and collagen coating on cell attachment to TICER® and pure titanium implant surfaces, Int. J. Oral Maxillofac. Surg. 37 (2008) 634–640. doi:10.1016/j.ijom.2008.01.021.

[29]   M.R. Kaluerović, J.P. Schreckenbach, H.-L.L. Graf, First Titanium Dental Implants with White Surfaces: Preparation and In Vitro Tests, Dent. Mater. 30 (2014) 759–768. doi:10.1016/j.dental.2014.04.005.

[30]   S. Abdi, M.S. Khoshkhoo, O. Shuleshova, M. Bönisch, M. Calin, L. Schultz, J. Eckert, M.D. Baró, J. Sort, A. Gebert, Effect of Nb addition on microstructure evolution and nanomechanical properties of a glass-forming Ti-Zr-Si alloy, Intermetallics. 46 (2014) 156–163. doi:10.1016/j.intermet.2013.11.010.

[31]   K. Zhuravleva, M. Bönisch, S. Scudino, M. Calin, L. Schultz, J. Eckert, A. Gebert, Phase transformations in ball-milled Ti-40Nb and Ti-45Nb powders upon quenching from the ß-phase region, Powder Technol. 253 (2014) 166–171. doi:10.1016/j.powtec.2013.11.002.

[32]   W. Xu, X. Wu, M. Stoica, M. Calin, U. Kühn, J. Eckert, K. Xia, On the formation of an ultrafine-duplex structure facilitated by severe shear deformation in a Ti-20Mo β-type titanium alloy, Acta Mater. 60 (2012) 5067–5078. doi:10.1016/j.actamat.2012.05.042.

[33]   A. Panigrahi, M. Bönisch, T. Waitz, E. Schafler, M. Calin, J. Eckert, W. Skrotzki, M. Zehetbauer, Phase transformations and mechanical properties of biocompatible Ti-16.1Nb processed by severe plastic deformation, J. Alloys Compd. 628 (2015) 434–441. doi:10.1016/j.jallcom.2014.12.159.

[34]   M.-L. Yen, C.-C. Chien, I.-M. Chiu, H.-I. Huang, Y.-C. Chen, H.-I. Hu, B.L. Yen, Multilineage differentiation and characterization of the human fetal osteoblastic 1.19 cell line: a possible in vitro model of human mesenchymal progenitors., Stem Cells. 25 (2007) 125–31. doi:10.1634/stemcells.2006-0295.

[35]   L. Crespo, M. Hierro-Oliva, S. Barriuso, V. Vadillo-Rodríguez, M.Á. Montealegre, L. Saldaña, E. Gomez-Barrena, J.L. González-Carrasco, M.L. González-Martín, N. Vilaboa, On the interactions of human bone cells with Ti6Al4V thermally oxidized by means of laser shock processing, Biomed. Mater. 11 (2016) 015009. doi:10.1088/1748-6041/11/1/015009.

[36]   A. Strzelecka-Kiliszek, L. Bozycki, S. Mebarek, R. Buchet, S. Pikula, Characteristics of minerals in vesicles produced by human osteoblasts hFOB 1.19 and osteosarcoma Saos-2 cells stimulated for mineralization, J. Inorg. Biochem. 171 (2017) 100–107. doi:10.1016/j.jinorgbio.2017.03.006.

[37]   V.N. Malheiro, R.L. Spear, R.A. Brooks, A.E. Markaki, Osteoblast and monocyte responses to 444 ferritic stainless steel intended for a Magneto-Mechanically Actuated Fibrous Scaffold, Biomaterials. 32 (2011) 6883–6892. doi:10.1016/j.biomaterials.2011.06.002.

[38]   V.N. Malheiro, J.N. Skepper, R.A. Brooks, A.E. Markaki, In Vitro Osteoblast Response to Ferritic Stainless Steel Fiber Networks for Magneto-active Layers on Implants, J. Biomed. Mater. Res. Part A. 101 (2013) 1588–1598. doi:10.1002/jbm.a.34473.

[39]   K. Anselme, P. Linez, M. Bigerelle, D. Le Maguer, a. Le Maguer, P. Hardouin, H.F. Hildebrand, a. Iost, J.M. Leroy, The relative influence of the topography and chemistry of TiAl6V4 surfaces on osteoblastic cell behaviour, Biomaterials. 21 (2000) 1567–1577. doi:10.1016/S0142-9612(00)00042-9.

[40]   J.E. Aubin, Bone Stem Cells, J. Cell. Biochem. Suppl. 30–31 (1998) 73–82.

[41]   M.P. Lynch, J.L. Stein, G.S. Stein, J.B. Lian, The Influence of Type I Collagen on the Development and Maintenance of the Osteoblast Phenotype in Primary and Passaged Rat Calvarial Osteoblasts: Modification of Expression of Genes Supporting Cell Growth, Adhesion, and Extracellular Matrix Mineralizatio, Exp. Cell Res. 216 (1995) 35–45.

[42]   P.F. Gostin, A. Helth, A. Voss, R. Sueptitz, M. Calin, J.J. Eckert, A. Gebert, Surface treatment, corrosion behavior, and apatite-forming ability of ti-45Nb implant alloy, J. Biomed. Mater. Res. - Part B Appl. Biomater. 101 B (2013) 269–278. doi:10.1002/jbm.b.32836.

[43]   H.J.J. Robinson, A.E.E. Markaki, C.A. a. Collier, T.W.W. Clyne, Cell adhesion to plasma electrolytic oxidation (PEO) titania coatings, assessed using a centrifuging technique, J. Mech. Behav. Biomed. Mater. 4 (2011) 2103–2112. doi:10.1016/j.jmbbm.2011.07.009.

[44]   W.K. Yeung, G.C. Reilly, A. Matthews, A. Yerokhin, In vitro biological response of plasma electrolytically oxidized and plasma-sprayed hydroxyapatite coatings on Ti-6Al-4V alloy, J. Biomed. Mater. Res. - Part B Appl. Biomater. 101 B (2013) 939–949. doi:10.1002/jbm.b.32899.

[45]   S.-D. Wu, H. Zhang, X.-D. Dong, C.-Y. Ning, A.S.L.L. Fok, Y. Wang, Physicochemical properties and in vitro cytocompatibility of modified titanium surfaces prepared via micro-arc oxidation with different calcium concentrations, Appl. Surf. Sci. 329 (2015) 347–355. doi:10.1016/j.apsusc.2014.12.039.

[46]   C.J. Kirkpatrick, V. Krump-Konvalinkova, R.E. Unger, F. Bittinger, M. Otto, K. Peters, Tissue response and biomaterial integration: The efficacy of in vitro methods, Biomol. Eng. 19 (2002) 211–217. doi:10.1016/S1389-0344(02)00019-9.

[47]   A. Palmquist, O.M. Omar, M. Esposito, J. Lausmaa, P. Thomsen, Titanium oral implants: surface characteristics, interface biology and clinical outcome., J. R. Soc. Interface. 7 Suppl 5 (2010) S515-27. doi:10.1098/rsif.2010.0118.focus.

[48]   A.K. Refai, M. Textor, D.M. Brunette, J.D. Waterfield, Effect of titanium surface topography on macrophage activation and secretion of proinflammatory cytokines and chemokines, J. Biomed. Mater. Res. A. 70 (2004) 194–205. doi:10.1002/jbm.a.30075.

[49]   M. Vandrovcova, I. Jirka, K. Novotna, V. Lisa, O. Frank, Z. Kolska, V. Stary, L. Bacakova, Interaction of human osteoblast-like Saos-2 and MG-63 cells with thermally oxidized surfaces of a titanium-niobium alloy, PLoS One. 9 (2014). doi:10.1371/journal.pone.0100475.

[50]   M. Martinesi, S. Bruni, M. Stio, C. Treves, F. Borgioli, In vitro interaction between surface-treated Ti-6Al-4V titanium alloy and human peripheral blood mononuclear cells, J. Biomed. Mater. Res. - Part A. 74 (2005) 197–207. doi:10.1002/jbm.a.30366.

[51]   R. Sabat, IL-10 family of cytokines, Cytokine Growth Factor Rev. 21 (2010) 315–324.

doi:10.1016/j.cytogfr.2010.11.001.

[52] K. Anselme, M. Bigerelle, Topography effects of pure titanium substrates on human osteoblast long-term adhesion, Acta Biomater. 1 (2005) 211–222. doi:10.1016/j.actbio.2004.11.009.

[53] E. Eisenbarth, D. Velten, M. Müller, R. Thull, J. Breme, Biocompatibility of β-stabilizing Elements of Titanium Alloys, Biomaterials. 25 (2004) 5705–5713. doi:10.1016/j.biomaterials.2004.01.021.

[54] O. Zinger, K. Anselme, A. Denzer, P. Habersetzer, M. Wieland, J. Jeanfils, P. Hardouin, D. Landolt, Time-dependent Morphology and Adhesion of Osteoblastic Cells on Titanium Model Surfaces Featuring Scale-resolved Topography, Biomaterials. 25 (2004) 2695–2711. doi:10.1016/j.biomaterials.2003.09.111.

[55] K. Anselme, M. Bigerelle, B. Noel, E. Dufresne, D. Judas, A. Iost, P. Hardouin, Qualitative and quantitative study of human osteoblast adhesion on materials with various surface roughnesses., J. Biomed. Mater. Res. 49 (2000) 155–66. http://www.ncbi.nlm.nih.gov/pubmed/10571901.

[56] H. Liao, A.-S.-. S. Andersson, D. Sutherland, S. Petronis, B. Kasemo, P. Thomsen, Response of Rat Osteoblast-like Cells to Microstructured Model Surfaces In Vitro, Biomaterials. 24 (2003) 649–654.

[57] P. Gupta, G. Tenhundfeld, E.O. Daigle, D. Ryabkov, Electrolytic plasma technology: Science and engineering-An overview, Surf. Coatings Technol. 201 (2007) 8746–8760. doi:10.1016/j.surfcoat.2006.11.023.

[58] H.P. Teng, C.J. Yang, J.F. Lin, Y.H. Huang, F.H. Lu, A Simple Method to Functionalize the Surface of Plasma Electrolytic Oxidation Produced TiO2 Coatings for Growing Hydroxyapatite, Electrochim. Acta. 193 (2016) 216–224. doi:10.1016/j.electacta.2016.02.060.

[59] L.H. Li, Y.M. Kong, H.W. Kim, Y.W. Kim, H.E. Kim, S.J. Heo, J.Y. Koak, Improved biological performance of Ti implants due to surface modification by micro-arc oxidation, Biomaterials. 25 (2004) 2867–2875. doi:10.1016/j.biomaterials.2003.09.048.

[60] Z. Huan, H. Yu, H. Li, M.S. Ruiter, J. Chang, I. Apachitei, J. Duszczyk, C.J.M. de Vries, L.E. Fratila-Apachitei, The effects of plasma electrolytically oxidized NiTi on in vitro endothelialization, Colloids Surfaces B Biointerfaces. 141 (2016) 365–373. doi:10.1016/j.colsurfb.2016.02.001.

[61] X.Z. Lin Zhu, Xun Ye, Guangxin Tang, Nanming Zhao, Yandao Gong, Yuanli Zhao, Jizong Zhao, Corrosion test, cell behavior test, and in vivo study of gradient TiO2 layers produced by compound electrochemical oxidation, J. Biomed. Mater. Res. Part A. 78A (2006) 515–522. doi:10.1002/jbm.a.

[62] M. Golozar, C.-E. Tanase, R. Brooks, S. Best, Extending the application of plasma electrolytic oxide coatings to novel low-rigidity beta-type titanium alloys: applications to load-bearing orthopaedic implants, Front. Bioeng. Biotechnol. (n.d.). doi:10.3389/conf.FBIOE.2016.01.00524.

[63] M. Bigerelle, K. Anselme, A kinetic approach to osteoblast adhesion on biomaterial surface, J. Biomed. Mater. Res. - Part A. 75 (2005) 530–540. doi:10.1002/jbm.a.30473.

[64] S. Endres, M. Wilke, P. Knöll, H. Frank, M. Kratz, A. Wilke, Correlation of in vitro and in vivo results of vacuum plasma sprayed titanium implants with different surface topography, J. Mater. Sci. Mater. Med. 19 (2008) 1117–1125. doi:10.1007/s10856-007-3086-6.